WILLIAM A. HUTING, JEFFERY W. WARREN, and JERRY A. KRILL

# RECENT PROGRESS IN CIRCULAR HIGH–POWER OVERMODED WAVEGUIDE

Several future Navy combat systems under development at APL require efficient delivery of high-power microwave energy from remote transmitters to phased-array antennas. To achieve this requirement, we have investigated the use of circular $TE_{01}$ mode "overmoded" waveguide technology. This effort has resulted in the invention of several new components, advancement of numerical modeling techniques, development and validation of new computer-aided-design computer programs, and the invention of several new fabrication techniques. The first application of this technology to a combat system element was recently achieved in the successful demonstration of the prototype Cooperative Engagement Capability, and steps toward a production military version of such a waveguide have been initiated.

## INTRODUCTION

Within several combat system development programs under way in APL's Fleet Systems Department, the need for efficient delivery of high-power microwave energy from advanced transmitters to phased-array antennas has been recognized. Future combat systems of the 1990s and future battle-force combatants into the next century will require the location of heavy power-conditioning and transmitting equipment below deck, thereby creating the potential for significant ohmic power loss and substantial risk of voltage breakdown (arcing) if conventional waveguide is used for future high-power levels.[1] Initial studies indicated that a form of "overmoded" waveguide could substantially reduce excessive loss and offer a substantial increase in power-carrying capacity without arcing. Naval shipboard, environmental, and high-power requirements had not been considered previously in overmoded technology, however.

In addition to accommodating substantial power transfer requirements, such waveguide could provide significant savings in system procurement cost. An example is the Cooperative Engagement Capability being developed under APL technical direction and tested on Aegis cruisers during August 1990. In this example, the Data Distribution System (DDS) requires efficient, high-power delivery to its phased-array antennas to meet specified antijamming performance. A standard waveguide run between the DDS transmitter and a mast-mounted array 150 ft away would result in the loss of nearly half the transmitter power. With overmoded waveguide, a reduction in loss to less than 10% could be realized in theory. In economic terms, the reduction in required transmitter equipment to achieve the same delivered power with overmoded waveguide was estimated to save at least $0.5 million per production unit.

From earlier APL studies, a feasibility project was initiated to determine if such waveguide could be designed and built. Combat system elements considered in the effort included the C-band DDS, S-band phased-array radar, and X-band missile fire-control systems. Table 1 lists the performance objectives of the overmoded waveguide for the three frequency bands considered.

We present the theoretical modeling and design, fabrication, and experimental results of circular–cross-section overmoded waveguide components invented and developed to support future combat system requirements. We also describe the concept and history of overmoded waveguide and discuss the theoretical modeling, prototype fabrication, and experimental results. Several transi-

**Table 1.** Objectives for experimental overmoded waveguide.

| Characteristic | S Band | C Band | X Band |
|---|---|---|---|
| Attenuation (dB/100 ft) | 0.10 | 0.17 | 0.30 |
| Peak power (MW, derated) | >6 | >0.1 | >1 |
| Cooling | Air | Air | Air |
| Weight | Comparable to rectangular waveguide with water cooling | | |
| Environment | Military rating for heat, shock, and vibration | | |

tion components had to be developed to allow the overmoded waveguide to be integrated into combat systems. They include compact elbows, transitions from rectangular to overmoded waveguide, unwanted-mode filters, and air-cooling inlets. These components are described, and preliminary results are presented as well. Finally, the current status of the technology is discussed, including progress toward technology transfer to industry.

## BACKGROUND AND HISTORY

Guided transmission of microwave and millimeter-wave electromagnetic signals of significant energy or requiring low loss has traditionally been accomplished with waveguide operating in transverse electric (TE) or transverse magnetic (TM) modes. Such waveguide has conventionally been designed for operation in the mode with the lowest cutoff frequency, $f_c$, within a frequency band below the cutoff frequencies of all other modes. Thus, signal energy cannot be coupled into other modes with different group velocities. Such energy transfer, if it did occur, would cause distortion and decrease coupling efficiency to other portions of the circuit. The design of conventional waveguide is straightforward, involving the selection of appropriate cross-sectional areas. Rectangular waveguide is the most widely used of this type.

Conventional waveguide is characterized by limits in maximum transmitted power and minimum wall attenuation, and both performance limitations result primarily from constraints on cross-sectional areas to ensure the cutoff of higher-order modes. To remove these limitations, waveguide can be designed to operate in an overmoded fashion in which a desired mode is favored and unwanted modes are suppressed by means other than operating below the cutoff frequencies of these modes. The idea of overmoded waveguide was conceived more than forty years ago,[2] and all but the desired mode were suppressed initially by tight cross-sectional and axial straightness tolerances and later by internal metallic or dielectric structures. Several different overmoded configurations, favoring different modes, have been investigated; [3,4] the configuration receiving the greatest attention, however, has been circular $TE_{01}$ mode waveguide. Figure 1 shows the electric and magnetic field lines of this mode. The circular $TE_{01}$ mode results in monotonically decreasing wall attenuation with increasing cross-sectional area, as shown in Figure 2.

The primary circular $TE_{01}$ mode waveguide application of interest in the past, for which the bulk of the theory was developed, was for low-loss transmission of many telecommunication channels between cities. Although much work was done at Bell Telephone Laboratories,[5,6] many organizations from various nations eventually joined the effort.[7] Favored approaches to the design of circular $TE_{01}$ mode overmoded waveguide provided continuous unwanted-mode decoupling and suppression via either a thin, low-loss-dielectric internal lining (i.e., lined waveguide), or an internal helix of insulated wire ensheathed in dielectric and enclosed in a conducting outer shell (i.e., sheathed-helix waveguide). Both configurations are shown in Figure 3. The operating band was at millimeter wavelengths, and frequencies

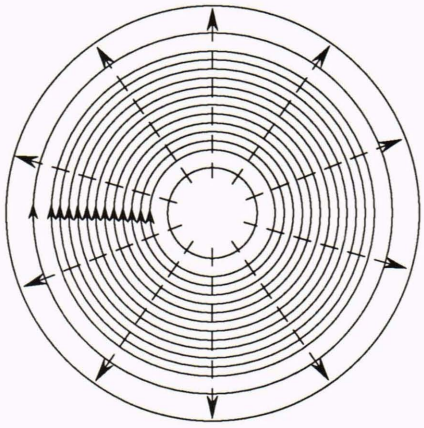

**Figure 1.** The electric field lines (solid curves) and magnetic field lines (dashed lines) of a circular $TE_{01}$ wave.

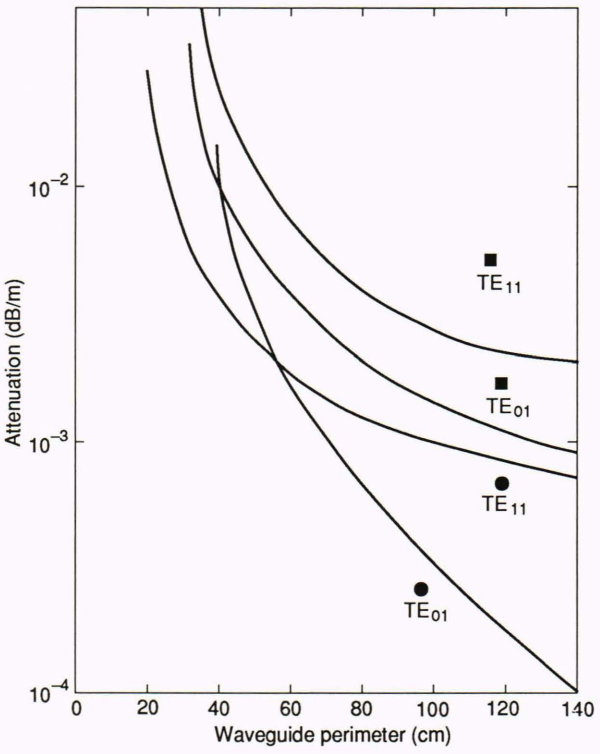


**Figure 2.** The attenuation of various circular and square waveguide modes as a function of waveguide perimeter.

ranged from 50 to 120 GHz. This design resulted in the requirement to suppress up to hundreds of unwanted modes for the 1- to 3-cm typical waveguide radii. Significant success with an experimental underground telecommunication trunk line was reported by the mid-

1970s.[7] After the advent of fiber optics, interest in overmoded waveguide for this application waned.

Other applications of circular $TE_{01}$ overmoded waveguide cited in the literature include wideband data transfer between elements of the very large array (VLA) radio telescope, use in microwave ground-to-satellite transmissions, microwave radar, energy insertion into fusion devices, and even a proposed approach for low-loss power transmission from generation sites.[8] Interest in the application of overmoded waveguide to high-power microwave and millimeter-wave radar and communication systems has been increased by recent advances in high-power sources such as gyrotrons and extended interaction klystrons.

## OVERMODED WAVEGUIDE

To achieve low transmission loss and high power-carrying capacity, it is often necessary to select a waveguide radius so large that operation occurs well above the $TE_{01}$ cutoff frequency. Consequently, such a system can support at least several propagating modes in addition to the four modes with cutoff frequencies less than or equal to the $TE_{01}$ cutoff frequency. The excitation of these extra modes can greatly increase transmission loss because of signal dispersion and matching problems at the receiver due to mode coupling. Sheathed-helix waveguide (Fig. 3) consists of a closely wound insulated wire surrounded by a layer of lossy dielectric that is encapsulated by a good conductor. It is well known that this configuration strongly suppresses and attenuates unwanted modes while preserving the desirable low-attenuation characteristics of the $TE_{01}$ mode. This behavior occurs because the insulated helix favors azimuthal currents characteristic of only $TE_{0m}$ modes. Suppression of $TE_{02}$ modes and higher can be accomplished with a guide radius restriction so that they are evanescent.

New design features presented here include high power-carrying capacity and severe spatial requirements that limit waveguide bend radii and waveguide diameter. This work has led to advances in theoretical modeling, fabrication techniques, and available components.

### Overmoded Waveguide Design Analysis

This section describes the design and development of circular overmoded waveguide, including straight sections and optimized bends with consideration of fabrication tolerances. Our efforts to date have concentrated on designs for the S (2–4 GHz), C (4–6 GHz), and X (10–12 GHz) bands. Appropriate design characteristics were selected after a lengthy parametric analysis. For example, the low-attenuation objective at S band requires a large waveguide radius, whereas the requirement for very compact 90° bends makes a small waveguide radius desirable. Further, because of the high-power objective, the mode-suppressing structures should be located in the vicinity of low electric field to reduce the possibility of electrical breakdown in the dielectric material. After it was determined that these requirements could, in principle, be satisfied by the $TE_{01}$ mode, computer programs were written for the configurations of Figure 3. The programs were based on theoretical developments by Unger and by Carlin and D'Agnostino, as summarized in Ref. 9, to predict transmission loss in straight and tapered curvature bend sections with parametric variations in dimensions and material properties. The sensitivity of transmission loss to waveguide dimensional tolerances within our design constraints was also analyzed by using Bell Telephone Laboratories work and extrapolating from it.[10]

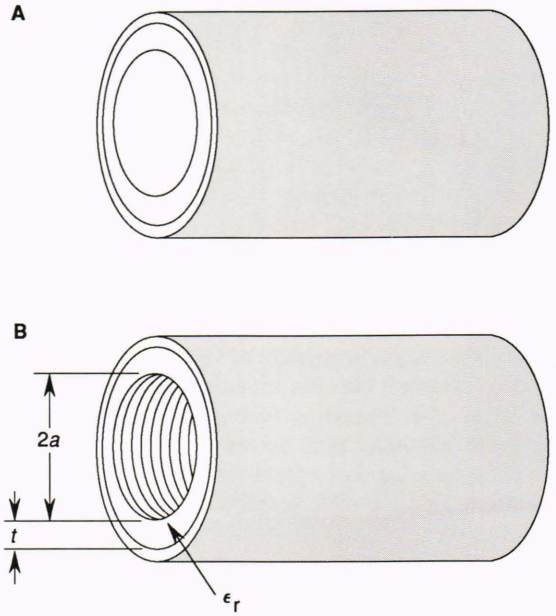


**Figure 3.** Two configurations for suppressing unwanted modes. **A.** Metallic waveguide with dielectric lining. **B.** Sheathed-helix waveguide. The term $a$ is the helix radius, $t$ is the lining thickness, and $\epsilon_r$ is the sheath relative dielectric constant. See Table 3 for values of the parameters for S, C, and X bands.

The principal loss mechanism due to overmoded $TE_{01}$ mode waveguide bending is given by

$$L = L_W + L_M + L_C , \qquad (1)$$

where $L_W$ is $TE_{01}$ mode attenuation; $L_M$ is added transmission loss caused by axial bending (mode distortion loss); and $L_C$ is added transmission loss caused by spurious mode excitation (mode conversion loss).

For helical waveguide, $L_W$ is given by the expression for the ohmic loss in a smooth continuous wall modified by an interwinding helix capacitance, and also by helix eddy current, pitch, and insulation losses. In our work, the calculated value of $L_W$ is equal to the smooth wall loss multiplied by a factor of 1.1. The mode distortion and conversion losses are given by the following approximate expressions, respectively:[9]

$$L_M = f_m \sum_{n=1}^{\infty} C_n^2 \, \Delta\alpha_n / (\Delta\beta_n)^2 , \qquad (2)$$

and

$$L_C = f_c \sum_{n=1}^{\infty} C_n^2/(\Delta\beta_n)^4 , \qquad (3)$$

where $C_n$, $\Delta\beta_n$, and $\Delta\alpha_n$ are the coupling coefficient, propagation constant difference, and the attenuation constant difference between the $TE_{01}$ mode and the $n$th unwanted mode (assuming $\Delta\alpha_n << \Delta\beta_n$), respectively. The variables $f_m$ and $f_c$ are functions of the bend geometry. Explicit expressions for these parameters, as well as the approximate complex mode eigenvalues on which they are based, are summarized in Ref. 9.

The expressions for transmission loss in Equations 1, 2, and 3 are for intentional (as opposed to random, within-tolerance) bending and have been used for highly overmoded millimeter band designs with very gradual bending over many wavelengths. Our applications involve sharp bends, which require certain modifications to the theoretical approximations used in deriving Equations 1, 2, and 3. First, for sharp bending over a few wavelengths, the approximation used by Unger for mode distortion loss (Eq. 2) is not strictly valid over the range of design parameters. Specifically, it was determined that for many of the designs considered by us, the gradual bend condition (allowing the approximation used in deriving Eq. 2) did not always hold, necessitating the numerical evaluation of a more general expression for $L_M$.

To confirm further that the theoretical design modeling is valid in our regime, we investigated an alternative approach using complex modal eigenvalues from more general expressions. The eigenvalues were found by using two methods (Newton's method and Muller's method), and the resultant data were in excellent agreement with the approach described earlier. About 1200 design parameter combinations were analyzed numerically not only for helix waveguide but also for lined waveguide (Fig. 3). The reason for considering lined waveguide was its simplicity and relative fabrication ease. Figure 4 shows sample results for a representative design of helix waveguide at S band. In these examples, total transmission attenuation for a representative run length (including one bend) versus waveguide cross-sectional radius is plotted, as is the attenuation of the bend itself. The bend length was optimized subject to size constraints typical of shipboard radar and radio communication systems. Following the procedure outlined by Unger,[6] the bend curvature profile shown in Figure 5 was considered to be linear. We were able to obtain a bend design meeting our objectives, in which the linear curvature taper corresponds to an elastic bend shape described by Fresnel integrals. Analysis yielded the empirical relationships for a design characterized by low bend attenuation and relatively compact bend length for a 90° linear curvature profile. These empirical results are summarized in Table 2.

Comparison of results revealed that the sheathed-helix waveguide is superior to lined waveguide in meeting

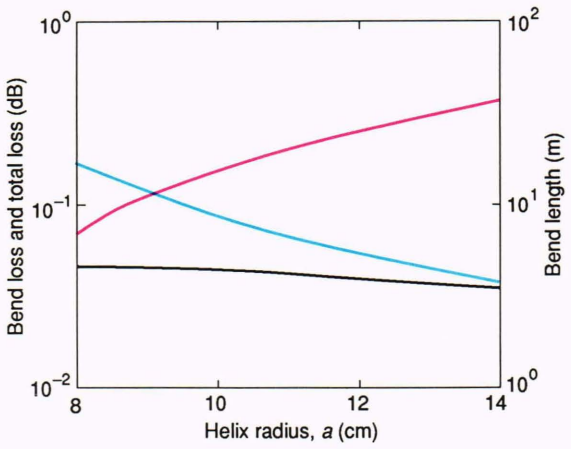


**Figure 4.** Characteristics of an optimum sheathed-helix waveguide run 150 ft long with one 90° bend. The bend loss (black), total loss (blue), and bend length (red) are plotted as a function of the helix radius. The sheath relative dielectric constant $\epsilon_r = 2.0 - j0.1$, and $\delta = t/a = 0.1$, where $t$ is the lining thickness and $a$ is the helix radius.

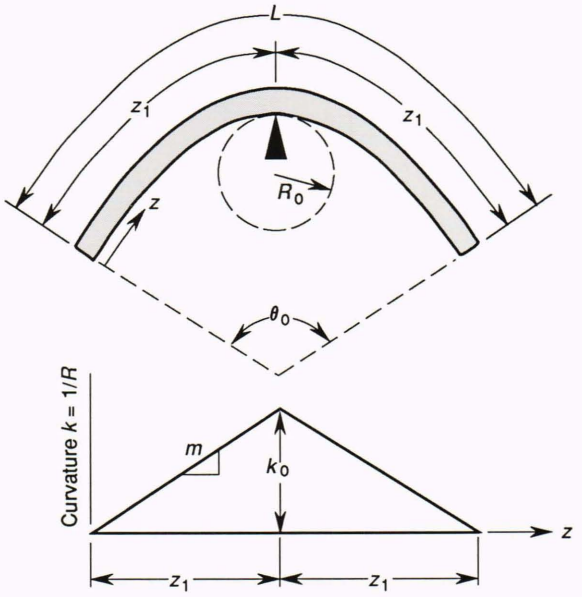


**Figure 5.** Waveguide bend geometry used in our work. $L$ is the length, where $L = 2z_1$; $R_0$ is the minimum bend radius; $\theta_0$ is the bend angle; $k_0$ is the reciprocal of $R_0$; and $R$ is the tangential radius of curvature of the bend. The inverse of $R$ is given by $k$, and $m$ is the derivative of $k$ with respect to the axial dimension $z$. See Table 4 for values of the parameters for the S, C, and X bands.

performance objectives, given the constraint that the same dielectric be used for both bend and most straight sections (for minimum reflections). The most advantageous lined waveguide designs were computed to have at least 3 times greater loss per bend and per total run length than the sheathed-helix design. Limited availability of practical dielectric materials meeting thermal and dielectric strength objectives further supports this conclusion, since lined waveguide dielectric is exposed to

higher electromagnetic fields. In contrast, the wire windings in the helix waveguide shield the lossy dielectric from high electric fields, thereby reducing the risk of field- or heat-induced dielectric breakdown at high power. The helix waveguide designs selected for experimental development are summarized in Tables 3 and 4; these three designs were optimized for S, C, and X bands.[11]

Another important design issue is insensitivity to manufacturing and installation imperfections. Unger[10] developed analytic expressions for added loss caused by cross-sectional deviations, deviations from straightness, helix irregularities, and discontinuities between sections. In his work, the imperfection was modeled as a zero-mean random process with exponential covariance (correlation). The variable $L_0$ (correlation length) may be roughly described as the range over which the deformation may be expected to take on similar values. Figure 6 shows, as a function of $L_0$, the root-mean-square random bend radius required to increase transmission loss by the indicated values for our S-band waveguide. These curves are shown for different wall designs, including the limit of perfect azimuthal conductivity and zero longitudinal conductivity at the waveguide wall (infinite wall impedance), and the limit of perfect conductivity in all directions (metallic waveguide). As discussed in the next section, our fabrication process yields excellent tolerances far tighter than the deformation sizes indicated in Figure 6.

**Table 2.** Computer-generated design rules for the best performance of a constrained-size sheathed-helix waveguide bend (linear variation in $1/R$, where $R$ = bend radius).

| Characteristic | Value |
|---|---|
| Inner diameter (ID) | 1.75 to 2 wavelengths |
| Ratio of bend length to ID | 16 to 17 |
| Sheath thickness | 7.5% to 10% of waveguide ID |
| Real part of sheath dielectric constant | 6 to 11 |
| Imaginary part of sheath dielectric constant | –0.005 to –0.05 |

**Table 3.** Characteristics of sheathed-helix waveguides built at APL.

| Parameter[a] | S band | C band | X band |
|---|---|---|---|
| $a$ (cm) | 8.0 | 6.0 | 3.0 |
| $t$ (cm) | 0.8 | 0.6 | 0.3 |
| $\epsilon_r$ | $5.2 - j0.052$ | $5.2 - j0.052$ | $5.2 - j0.052$ |
| $f_{op}$ (GHz) | 3.0–4.0 | 4.0–5.0 | 10.0–11.0 |

[a]The parameters are illustrated in Figure 3; $a$ is the helix radius, $t$ is the lining thickness, $\epsilon_r$ is the sheath relative dielectric constant, and $f_{op}$ is the operating frequency.

**Table 4.** Design characteristics for our bends. The S band and X band bends have been built and tested.

| Parameter[a] | S band | C band | X band |
|---|---|---|---|
| Minimum bend radius $R_0$ (ft) | 2.46 | 1.82 | 0.82 |
| Length $L = 2z_1$ (ft) | 7.73 | 5.73 | 2.6 |
| $\theta_0$ (deg) | 90 | 90 | 90 |

[a]The parameters are illustrated in Figure 5.

## Sheathed-Helix Waveguide Fabrication

Fabrication processes have been developed and exercised by members of APL's Fleet Systems and Technical Services Departments. The techniques used were developed with the goal of fabricating compact, low-loss, high-power, overmoded waveguide components by using techniques that demonstrate that cost-effective production is possible.

Figure 7 is a photograph of a helix waveguide designed for C-band operation. The inner surface is formed with a tightly wound helix of insulated wire, which is surrounded by a lossy dielectric sheath made of a room-temperature vulcanizer (RTV). The final component is an aluminum tube that serves as a conducting shield and a mechanical structure. The key steps in fabricating straight sections of a helix waveguide will now be discussed.

The first step is to wind insulated wire around a mandrel to form the helix. The mandrel provides a cylindrical surface of the proper diameter to wind the wire and is removed at the completion of the fabrication process. Because the wire helix is under tension, a solid mandrel would be difficult to remove without damaging the waveguide. For this reason, the mandrel is built in six pieces that provide an accurate cylindrical surface when

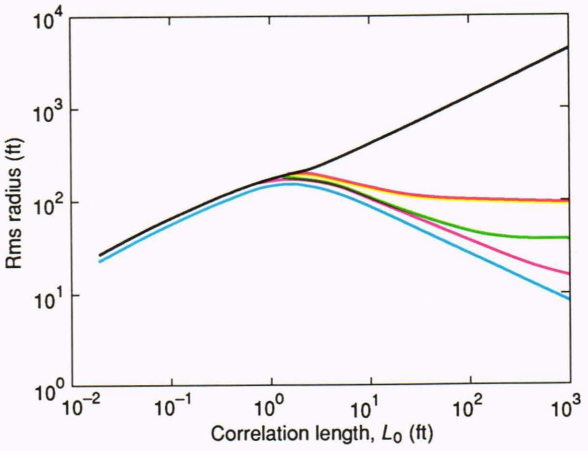


**Figure 6.** Root-mean-square random bend radius required to increase loss by a value equal to 10% of the plain copper waveguide loss for the $TE_{01}$ mode. The helix radius $a$ = 8.09 cm, and losstan is the loss tangent of the sheath material. Metallic waveguide (black), infinite wall impedance (blue), losstan = 0.001 (red), losstan = 0.010 (green), and losstan = 0.100 (orange).

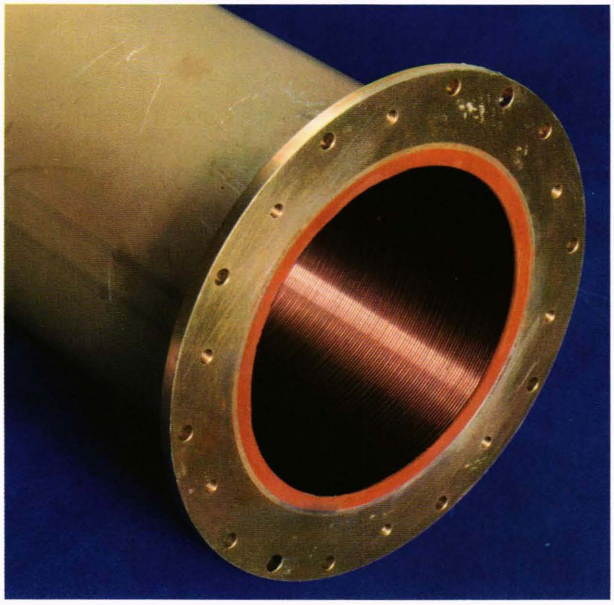

**Figure 7.** C-band sheathed-helix waveguide.

assembled, but it can be mechanically collapsed to extract the mandrel after assembly. The design of the mandrel is shown in Figure 8.

After the wire helix is wound onto the mandrel, we coat it with a thin layer of an RTV that adheres well to the wire. This adhesion is critical because the wire helix must eventually be held in place in the completed waveguide by its adhesion to the sheath (via the intermediate layer of RTV). The sheath material is a different type of RTV chosen for its electrical and thermal properties, as described previously. Because the intermediate layer of RTV is very thin, its electrical properties are relatively unimportant.

An aluminum tube serves as the outer shield for the overmoded waveguide. Because the desired mode is supported within the wire helix rather than within the aluminum tube, the dimensional tolerances of the aluminum tube are not stringent. Standard tolerances for commercial aluminum tubing are adequate. Flanges are welded onto the tubes and provide a convenient reference for aligning the tube during the assembly process.

The mandrel assembly (with wound wire and intermediate layer of RTV) is then inserted into the center of the aluminum tube in preparation for pumping in the sheath material (moderately lossy RTV). The sheath RTV is mixed with a catalyst that causes it to harden and is then pumped into the space between the wound wire and the aluminum tube. After the RTV has hardened, the assembly is removed from the pump, and the mandrel is collapsed and removed. The helix waveguide is now complete.

We have also fabricated helix waveguide bends. Although the process for fabricating helical bends is somewhat similar to fabricating straight sections, several differences make bend fabrication more difficult. The principal difficulty is a result of the fundamental requirement to use a nonuniform radius of curvature to achieve a high-performance compact bend. We fabricate 90° S-band bends by building two identical 45° bends that are joined to form a 90° bend.

The mandrel for fabricating bends is cast of a low–melting-temperature metal (called cerrometal) in a mold. To minimize the volume of cerrometal required and to provide mechanical strength, the cerrometal is cast over a metallic core that takes up most of the volume of the mandrel. The mold for this mandrel was machined to high tolerances (five-thousandths of an inch) with a numerically controlled milling machine in the Technical Services Department. Tight tolerances are required because the mandrel will define the shape of the inner surface of the waveguide. Since the inner surface (the helix) supports the mode of interest, failure to maintain tight tolerances will result in increased loss in the bend. A plastic coating is sprayed on the cerrometal before winding the wire on the mandrel. This coating helps to remove all of the cerrometal after the bend is complete.

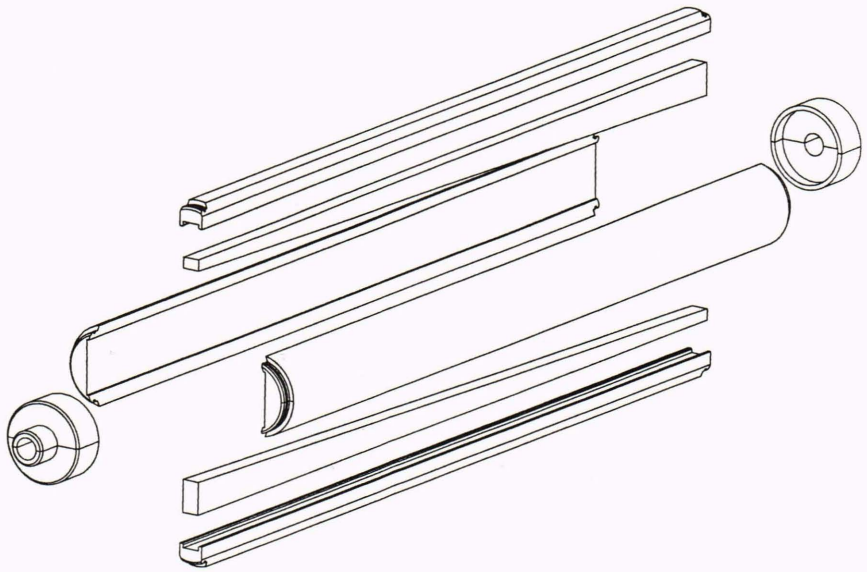

**Figure 8.** Mandrel used for wire wrapping.

Because the mandrel is not straight, a special patented fixture[12] is required to wind the wire. The wire winder invented for this task permits the wire to be wound on the curved mandrel with constant tension. Figure 9 shows the wire winder in operation for half of an S-band bend. An adjustment is provided to maintain the center of gravity of the wire winder as wire is transferred to the mandrel. After the wire is wound, it is coated with a thin layer of RTV in the same manner as the straight sections.

Because of its nonlinear curvature, the mandrel assembly cannot be inserted into an appropriately curved tube. Instead, the RTV is injected around the mandrel assembly within a two-piece mold. Figure 10 shows the assembly for a full 90° X-band bend after the RTV has hardened, with one-half of the mold removed. After the assembly (mandrel, wire, and RTV) is removed from the mold, flanges are fitted to each end, and aluminum tape is wrapped around the RTV to provide the outer shield. Two layers of fiberglass are then applied outside the aluminum tape to provide mechanical strength.

The next step is to remove the mandrel from the assembly by running hot water through the center of the mandrel to melt the cerrometal, which melts at 136°F. After the cerrometal is melted and has run out of the waveguide, the solid core of the mandrel is removed. The plastic layer described earlier can then be removed, bringing with it most of the remaining cerrometal. Direct application of hot water is usually required at this point to remove the final small quantities of cerrometal. Figure 11 shows a completed S-band bend.

We continue to investigate new techniques for fabrication of helical waveguide. A design has been completed for a collapsible mandrel that can be used to fabricate helical bends. This approach will eliminate the low–melting-temperature metal from the process, a source of most manufacturing difficulties.

## Experimental Results

In this section, test results are presented for straight helix waveguides and a helix waveguide bend. In many of the S-band measurements, low-power responses were observed by using a network analyzer. In these experiments, the test waveguide was excited by an incident $TE_{01}$ circular wave through the use of rectangular-to-circular waveguide transitions. The waveguide transition used in tests, invented by Marie,[13] is shown in Figure 12 (fabricated by APL). The tests can be divided into two categories: scattering parameter tests to determine insertion loss and reflectivity, and cavity tests to evaluate the suppression of unwanted modes.

Both straight sections and bends of helix waveguide were tested at S band and X band. It was concluded that the sheathed-helix waveguide and waveguide transitions are well matched; however, the helix waveguide attenuation is so low (e.g., a theoretical value of 0.003 dB/m at S band) that direct measurements of insertion losses of short lengths are not feasible and indirect methods are necessary.

To overcome this difficulty, a section of waveguide can be made into a variable-length cavity by placing a conducting plate at one end of the waveguide and by inserting a conducting piston into the other end. Karbowiak[14] published a relationship that expresses the attenuation per unit length $\alpha$ as a function of the quality factors ($Q$'s) and associated resonant cavity lengths $L$ for a fixed frequency:

$$\frac{1}{Q} = \frac{\lambda_0^2}{\pi\lambda_g}\left(\alpha + \frac{C}{L}\right), \tag{4}$$

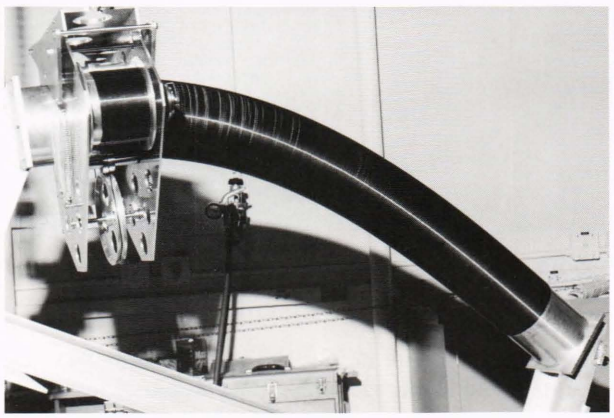

**Figure 9.** Wire-wrap device and waveguide bend mandrel.

**Figure 10.** Waveguide bend mandrel assembly.

**Figure 11.** S-band sheathed-helix waveguide bend.

**Figure 12.** X-band Marie transition made at APL.

where $\lambda_0$ is the free-space wavelength, and $\lambda_g$ is the wavelength in the waveguide. Thus, from a set of $Q$ measurements versus cavity lengths, a value for the insertion loss may be computed. This calculation was done for different short sections of straight S-band waveguide. Measurements on the most recently manufactured waveguide sections indicate attenuations with an upper bound of 0.005 dB/m; the theoretical value for a perfect waveguide is 0.003 dB/m. The insertion loss of the S-band 90° bend was computed by using a cavity configuration similar to the straight section. The insertion losses computed from these data agreed with the theoretical value to within 5%. Cavity tests also showed unwanted-mode suppression comparable to single-mode conventional waveguide to within the limits of our instrumentation (at least 40-dB suppression).

In addition to the low-power attenuation experiments, initial power capacity testing was performed. The predicted power capacity of circular overmoded waveguide at the 8-cm S-band radius, assuming a power derating factor of 5 and only slight pressurization, is 16 MW. In contrast, rectangular waveguide could not support such peak power without parallel reduced-power runs with combining circuitry, water cooling, and multiple-atmosphere pressurization with breakdown-resistant gas such as $SF_6$. Initially, a resonant ring waveguide configuration was built by Raytheon under APL subcontract to generate 5 MW of peak power at S band. With only slight overpressure, the helix waveguide exhibited no breakdown, as predicted. Similar helix waveguide optimized for the range of frequencies between 4 and 6 GHz (C band) has been tested to 10-kW average power. The C-band waveguide used an artificial sheath dielectric developed by Cumming Corporation to APL specifications with significantly lower weight (and dielectric strength) than that used in the S-band waveguide.

## OTHER REQUIRED COMPONENTS

Previously, we described how circular $TE_{01}$ mode overmoded waveguide of a sheathed-helix design was newly optimized for application to the microwave bands with high-power and low-attenuation requirements and subject to bend and cross-sectional constraints. Unfortunately, most microwave power sources and receivers are compatible with $TE_{10}$ rectangular waveguide rather than with circular waveguide, necessitating the use of metallic mode-transitioning waveguide sections. We will later describe a new metallic waveguide transition between one circular overmoded waveguide and four single-mode rectangular waveguides. One interesting application of this device is that, by inserting four rectangular bends between two of these transitions, a high-power-capacity elbow may be formed. Because this elbow has a small radius of curvature, it is better suited to severely space-constrained applications than are the more gentle circular overmoded bends described earlier. Another type of mode-transitioning elbow has also recently been invented and built; the fabrication of both types of elbows is presented later, as well as analytical techniques for use in evaluating such devices. The purposes of these transitions include matching both the desired $TE_{01}$ mode (for low loss) and all unwanted modes (for efficient coupling into unwanted-mode suppressing sections).

### Mode Transitions

We have fabricated and tested both the Marie and the multiport transition mentioned earlier to match circular overmoded waveguide with one or more runs of standard rectangular waveguide. The Marie transition has one rectangular port and one circular waveguide port. The multiport transition has four rectangular ports (for increased power capacity) and one circular waveguide port.

Figure 12 shows a Marie transition designed and built at APL for operation at X band. To achieve good performance, the inner surfaces of the Marie transducer must be fabricated accurately and with a very good surface finish by using a high-conductivity metal. Because of the complex shape and relatively small end openings, it is impractical to machine or to extrude such a part directly. Rather, a mandrel must be prepared, which can then be used with some type of molding or casting process to build the desired part.[4,13] We have built each of our mandrels from one piece of aluminum with a numerically controlled milling machine. After machining, the part is hand-polished to a high finish. The completed mandrel is then coated by electroforming. In the electroforming process, a very thick layer of copper is deposited on a mandrel, after which the mandrel is removed from the completed part. The copper layer is thick enough to provide a solid mechanical structure (we usually use a wall thickness of 1 to 2 mm). By carefully controlling the deposition conditions, the copper can be deposited with very low stress, resulting in excellent dimensional reproduction of the mandrel. In addition, the surface finish of the completed part is the same as the surface finish of the mandrel, which is critical for our application. An additional capability provided by electroforming is that the flanges for the transducer can be placed on the mandrel before electroforming and grown onto the transducer during the electroforming process. This feature provides excellent alignment of the flanges and a strong, low-cost joint. Because of the complex shape of the Marie transition, the mandrel cannot be removed mechanically. Rather, it must be etched away chemically,[4,13] leaving the completed Marie transition.

One critical issue in the design of waveguide transitions is power-carrying capacity. Taking full advantage of high-power-capacity overmoded waveguide requires a means for power insertion into, and extraction from, components of lower capacity. To provide high power to circular $TE_{01}$ mode waveguide from rectangular $TE_{10}$ mode waveguide via a transition such as the Marie transition would require substantial pressurization and cooling; the total power capacity is ultimately limited to that of the rectangular waveguide and transition. The use of several rectangular waveguides to feed a single overmoded waveguide increases power capacity in proportion to the number of rectangular feed ports. The new multiple-port rectangular $TE_{10}$ to circular $TE_{01}$ mode transition[15] is shown in Figure 13 for four rectangular feeds. The principal new element of the multiport transition is an inner pyramidal structure; the base is formed by the

inner walls of the rectangular waveguides where they begin to connect, and the tip occurs where the waveguides finally merge into a single cruciform cross section before the transition to the circular cross section. The internal edges and pyramid tip occur where the electric field is nearly zero and are rounded to a small radius to minimize the possibility of voltage breakdown. Proper phasing of the rectangular ports, for example, from separate, equal-amplitude, phase-aligned microwave sources, has been theoretically and experimentally verified to couple energy efficiently into the circular waveguide.

We now describe progress in manufacturing these multiport transitions. Since this was a new APL invention, our first effort to fabricate multiport transitions was directed toward building a highly flexible breadboard transition able to test numerous configurations quickly. Size and weight were not concerns for this breadboard. We decided to fabricate the breadboard from five pieces, which were machined from aluminum. The center pyramidal plugs were interchangeable to permit rapid testing of different configurations. Unlike the Marie transducer, the multiport transition can be fabricated in sections without sacrificing high-power capacity because the mechanical joints are placed in regions of low electric field. We have also built multiport transitions with slightly different designs by using sheet metal techniques (Fig. 13). These multiport transitions have undergone low-power microwave measurements. Measured attenuation and reflection compare favorably with theoretical results at S band. By measuring the transmission coefficient, $S_{21}$, of two such transitions back-to-back, the insertion loss was determined to be comparable with a pair of well-constructed Marie transitions.

## Mode-Transitioning Elbows

Whereas the helix waveguide bends described previously provide highly desirable performance characteristics for a bend (low loss and high power capacity), they are relatively expensive to fabricate and are still not as compact as may be required in some instances. For situations where somewhat higher insertion losses are acceptable, compact bends have been invented by using mode transitions.[16] The compact bend based on the multiport transition requires custom rectangular waveguide bends in addition to the transitions themselves. These bends can be fabricated with standard rectangular waveguide technology but require strict tolerances on the length to ensure proper phasing of the four legs (Fig. 14).

The principal challenge in the design of the elbow was to provide equal phase length and to interconnect rectangular waveguide bends properly between the four ports of each transition. As depicted in Figure 14, these

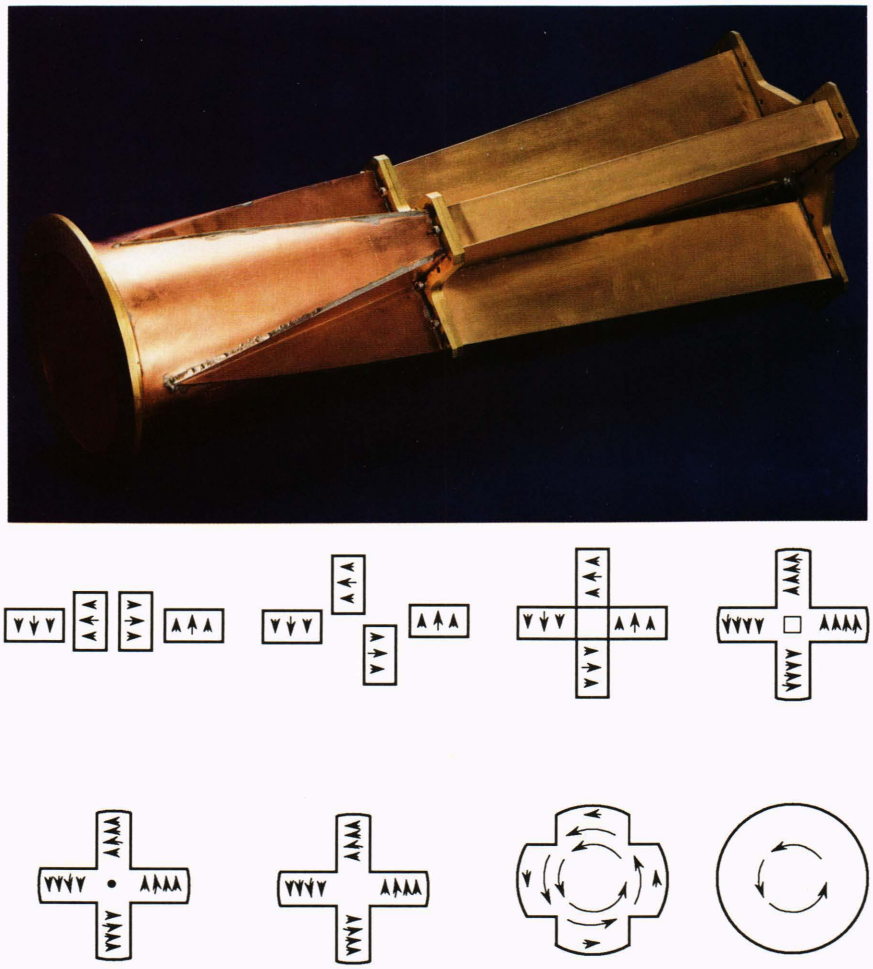

**Figure 13.** Multiport transition (top) along with desired electric field lines (bottom).

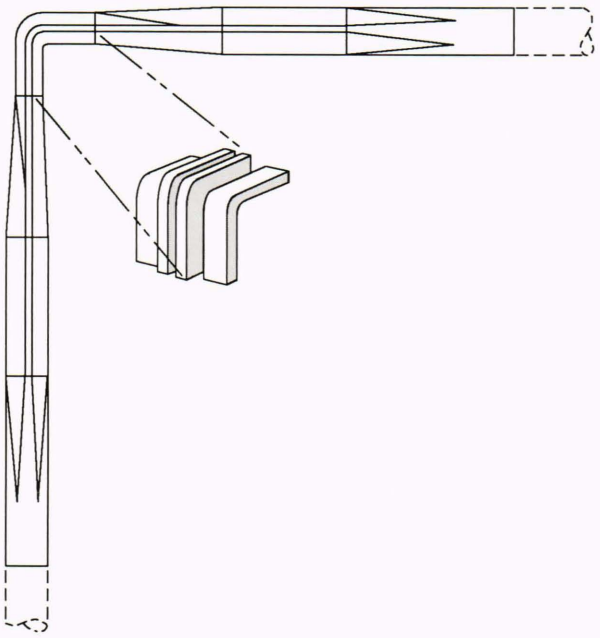

**Figure 14.** A waveguide elbow consisting of four tight $TE_{10}$ rectangular waveguide bends inserted between two multiport transitions.

requirements can be met by aligning the four rectangular waveguide ports so that their axes are in a common plane, and so that the two inner bends are in the *H* plane and the two outer bends are in the *E* plane. The rectangular waveguides emerge from the bend and are connected to the second multiport transition in the same manner as the connection to the first transition to preserve relative polarization in each port. Fabrication of the elbow is in progress.

A second compact bend invented at APL is shown in Figure 15. The mode transition consists of the portion of a Marie transition converting the circular $TE_{01}$ mode to the rectangular $TE_{20}$ mode. For the rectangular $TE_{20}$ mode, an *E*-plane bend can be very compact since the waveguide is not overmoded in that direction. Because part of the Marie transition has been eliminated from this bend, it has been measured to have lower loss than a Marie-based bend consisting of two complete Marie transitions and one rectangular waveguide elbow; it is also considerably smaller. In addition, because the eliminated portion of the Marie transducer usually constrains the power-handling capability of the device, the new bend has more power-handling capability than a Marie-transition–based bend.

## Numerical Evaluation of Waveguide Transition Designs

In the previous section, we discussed the fabrication and testing of waveguide transitions. Design objectives for these transitions include low mode-conversion loss and high power-carrying capacity. To achieve these goals, it was necessary to develop and validate a theoretical model of waveguide transition operation.

One of the earliest theoretical treatments of nonuniform waveguides (such as mode transitions) was given by Reiter,[17] who used the well-known fact that uniform waveguide modal fields form a complete orthogonal basis for physically realizable electromagnetic fields in a waveguide. Extending this concept to waveguide transitions, he asserted that the transverse electromagnetic field (*x* and *y* components) could be written as a sum of the transverse fields of the uniform modes corresponding to the local waveguide transition cross section:

$$\mathbf{E}_t(x, y, z) = \sum_{m=1}^{\infty} V_m(z)\mathbf{e}_m(x, y, z) , \tag{5}$$

$$\mathbf{H}_t(x, y, z) = \sum_{m=1}^{\infty} I_m(z)\mathbf{h}_m(x, y, z) , \tag{6}$$

where $\mathbf{E}_t$ is the transverse electric field, $\mathbf{H}_t$ is the transverse magnetic field, $\mathbf{e}_m$ is the transverse electric field of the *m*th uniform waveguide mode (suitably normalized), $\mathbf{h}_m$ is the transverse magnetic field of the *m*th uniform waveguide mode (suitably normalized), $V_m(z)$ is the so-called equivalent voltage, and $I_m(z)$ is the so-called equivalent current.

The equivalent voltages and currents are determined by an infinite set of ordinary differential equations that include both TE and TM modes:

$$\frac{dV_m}{dz} = -j\beta_m Z_m I_m + \sum_{n=1}^{\infty} T_{mn} V_n , \tag{7}$$

and

$$\frac{dI_m}{dz} = -j\frac{\beta_m}{Z_m} V_m - \sum_{n=1}^{\infty} T_{nm} I_n . \tag{8}$$

The variable $\beta_m$ denotes the wave number of the *m*th mode, $Z_m$ denotes the wave impedance of the *m*th mode, and the transfer coefficients $T_{mn}$ (which describe coupling between the two modes *m* and *n*) are given by

$$T_{mn}(z) = \int\int \frac{d\mathbf{e}_m}{dz} \cdot \mathbf{e}_n \, dx \, dy . \tag{9}$$

The integration is over the local waveguide cross section. Equations 7 and 8 are known as the generalized telegraphist's equations. By truncating the series in Equations 7 and 8, the equations are cast into a form amenable to numerical techniques. By using these techniques, a

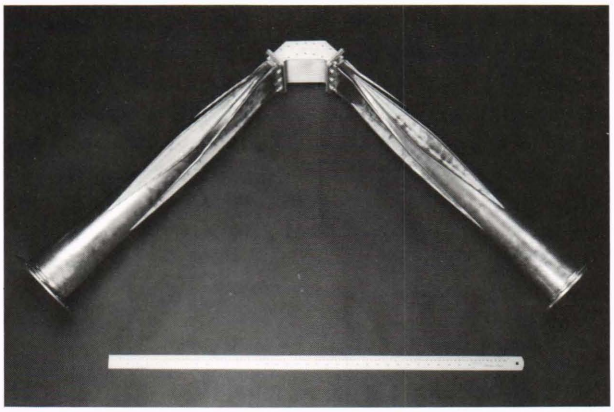

**Figure 15.** Waveguide elbow consisting of a tight $TE_{20}$ rectangular waveguide bend inserted between two transitions.

computer-aided-design program for Marie transitions was developed at APL[18–20] and by others,[21] and a similar program for multiport transitions will be developed. In implementing these programs, we have found that the tasks requiring the most programming effort and computer time are the determination of the coefficients in Equations 7 and 8. The major prerequisite for the computation of these variables is to calculate the modal fields of Equation 5, to integrate the scalar product of these fields according to Equation 9, and to obtain numerical values for $\beta_m$ and $Z_m$. One procedure that does these things numerically is the finite-element method (FEM). Of the available techniques, this appears to be the one that can best approximate a complicated boundary for a given number of nodes.[18]

To run FEM, it is necessary to approximate the waveguide cross section as a union of triangles. The scalar field potentials are then approximated as a sum of Lagrange interpolation polynomials. For the large number of waveguide cross sections treated in this work, the triangle-generating process is complicated and formidable. Software that generates such triangles was procured from Los Alamos National Laboratory and installed on the APL Amdahl system. This triangle generator, or mesh generator, is part of a finite-difference package called POISSON/SUPERFISH, which was developed for the Department of Energy to solve magnetostatic/electrostatic problems and RF cavity problems.[22]

The first step in the analysis of a waveguide transition with arbitrary cross sections is to solve the uniform waveguide problem for some large number $M$ of transition cross sections (Fig. 16). The vector functions $\mathbf{e}_m$ can be found by taking the gradient of the solutions to the scalar Helmholtz equation. In the case of the Marie transducer, this transverse differentiation may be avoided. As observed by Saad et al.,[23] only the circular $TE_{01}$, circular $TE_{41}$, circular $TE_{02}$, circular $TE_{42}$, and so on, modes are active in the device. It can be shown that, because only TE modes are involved, one may rewrite Equation 9 by using scalar potentials. These scalars must be numerically differentiated with respect to $z$, however.

The implementation of these steps for two identical X-band Marie transitions fabricated by APL is described in detail in Ref. 18. Figure 17 shows both numerical and

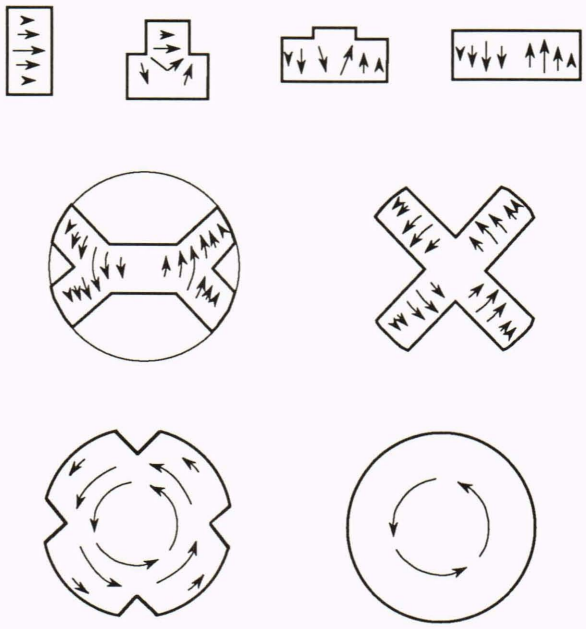

**Figure 16.** Cross sections of the Marie transitions shown with the electric field lines of the desired mode.

experimental data for the two X-band Marie transitions fabricated by APL that are connected by a short circular waveguide.[18] Agreement is good within present uncertainties of ohmic loss (under investigation). Low mode-coupling loss is evident for this design in both prediction and experimental results, a critical feature to successful designs.

Future work in this area consists mainly of implementing a similar program set for the multiport transition. The four waveguide modes of chief concern are the desired $TE_{01}$ mode, the unwanted $TE_{21}$ mode, and two orthogonal polarizations of the unwanted $TE_{12}$ mode (Fig. 18). The unwanted modes might be generated when, for example, the rectangular ports are being used as inputs, that is, power flows from the rectangular ends to the circular ends, and the rectangular inputs are of different magnitudes or phases, or if one of the ports shuts down temporarily, for example, because of arcing. It is important to determine the sensitivity of signal matching the rectangular ports to ensure satisfactory performance.

## Matched Unwanted-Mode Filter

The sheathed-helix waveguide design described earlier provides significant continuous suppression of unwanted modes along its length. To provide further suppression near transitions for high-power system applications requiring high spectral purity of the signals, a new helix waveguide mode filter has been invented to match both the desired $TE_{01}$ mode and the undesired modes. The $TE_{01}$ mode is passed with minimal attenuation, but the unwanted modes are absorbed. Figure 19 illustrates the characteristics of the filter, shown inserted between a metal transition and a length of sheathed-helix waveguide. A gradual change in sheath dielectric loss tangent occurs along the filter from the helix waveguide to the transition. The gradual change is accomplished by join-

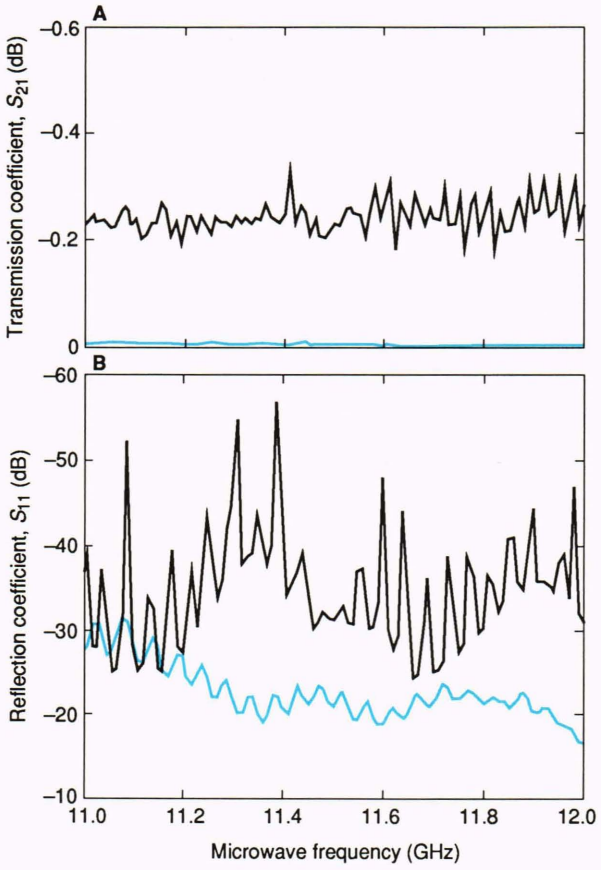


**Figure 17.** Experimental (black) and numerical (blue) data for two Marie transitions connected by a circular waveguide for microwave frequencies between 11 and 12 GHz. **A.** Transmission loss. **B.** Reflectivity. In Part **A**, the experimental data include both mode coupling loss and ohmic loss, whereas the numerical data include mode coupling loss only.

ing male and female conic sections of low-loss and high-loss sheath material, as illustrated in Figure 19.

## INTERNAL AIR COOLING

Because of its low attenuation, overmoded helix waveguide can support high average power yet requires only minimal cooling. The potential difficulty lies in the principal heating that would occur at the internal helix. If the dielectric sheath is not sufficiently thermally conducting, then internal air cooling within the helix is necessary. Figure 20 is a plot of internal air-cooling heat dissipation versus airflow speed for 170 W of heating per meter of waveguide length, assuming thermal insulation from the outside wall in the worst case. This heat loss corresponds to an average waveguide power of about 200 kW. Numerical modeling for both laminar and turbulent airflow was performed; moderate turbulent airflow maintained acceptably low waveguide temperature.

Insertion and extraction of cooling air must be accomplished without disrupting the overmoded field pattern. Because of the relative insensitivity of the $TE_{01}$ mode to wall imperfections, a fine copper mesh-screen waveguide with good radius tolerance comparable to that of the equal-radius helix can be inserted between helix

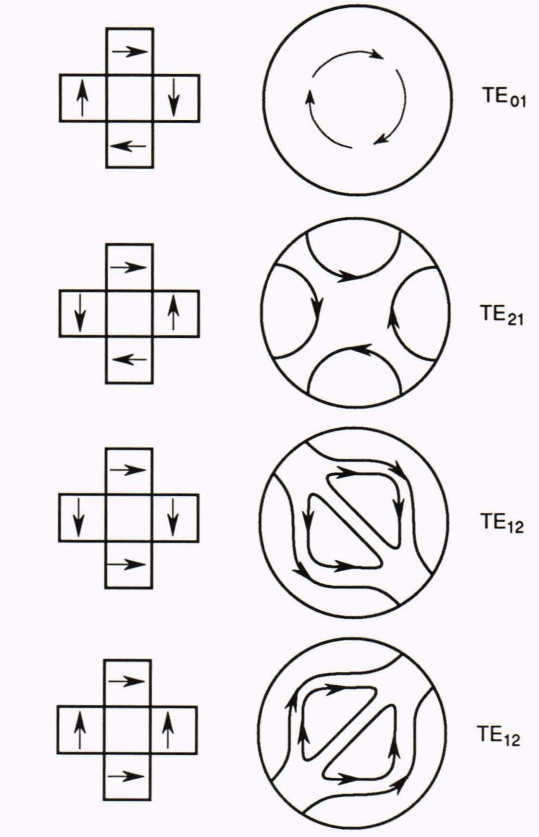


**Figure 18.** Waveguide modes in multiport transition.

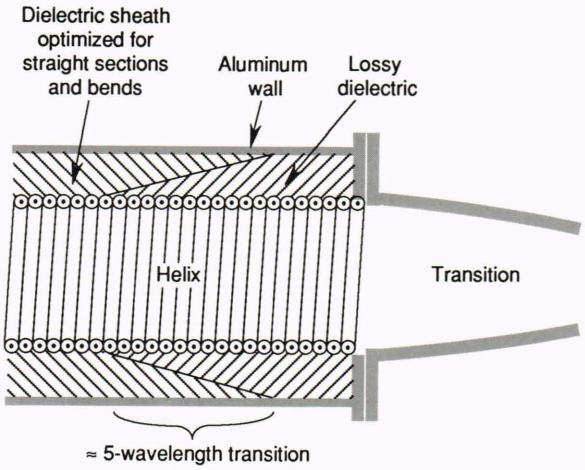


**Figure 19.** Design characteristics of a matched unwanted-mode filter.

waveguide or matched filter sections. Air is inserted or extracted through the screen section. Alternatively, a perforated helix waveguide section was invented, consisting of an internal metal screen of azimuthal inner wall conductivity. As shown in Figure 21, the dielectric sheath is perforated, and the outer conductor is an aluminum screen. Although more difficult to construct, the latter approach maintains continuous mode suppression.[24]

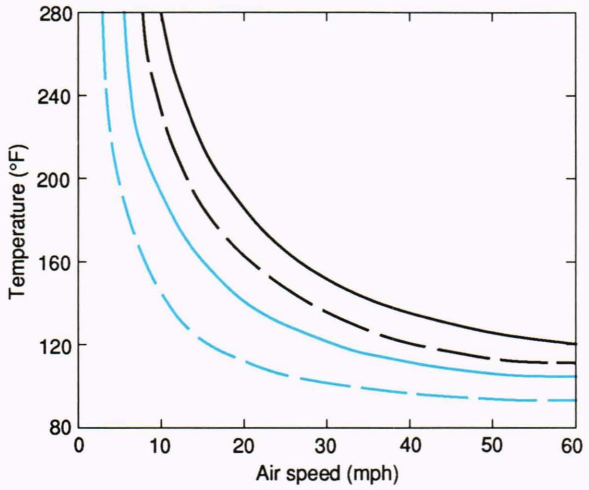


**Figure 20.** Temperature versus air speed for 150-ft waveguide run with one bend (S band). At the entrance, the pressure was 1 atm and the temperature was 81°F. The average power was 225 kW, and 7.7-kW loss = 51 W/ft. The solid curves are plots of the highest temperature in the bend, and the dashed curves are plots of the exit temperature in the bend waveguide wall. Internal flow (black curves) assumes all heat was dissipated on the insulated inner wall, and external ducted flow (blue curves) assumes all heat was dissipated on the insulated outer waveguide wall.

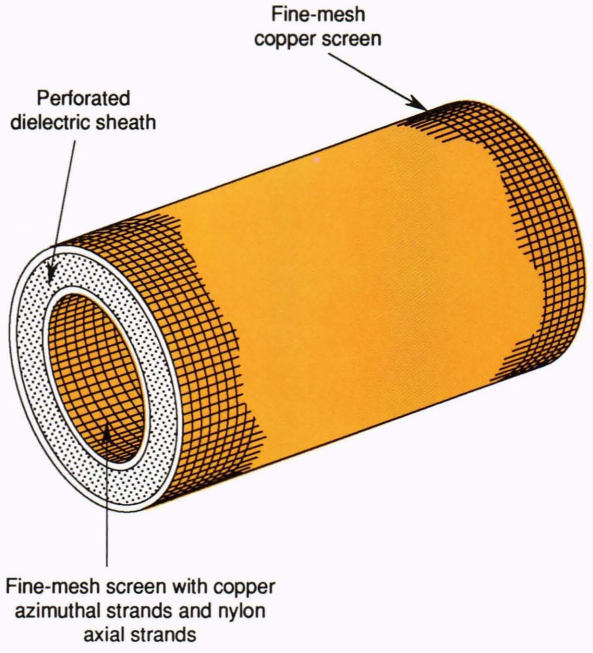


**Figure 21.** Helix air-cooling inlet.

## SUMMARY AND FUTURE WORK

Circular $TE_{01}$ mode overmoded waveguide of a sheathed-helix design has been newly optimized for application to microwave bands subject to high-power and low-attenuation objectives and to bend and cross-sectional size constraints. New circular $TE_{01}$ mode components have also been described that provide further design flexibility for high-power waveguide systems. The multiple-port rectangular $TE_{10}$ to circular $TE_{01}$ mode waveguide transition provides division of power from larger-diameter, higher-power-capacity $TE_{01}$ mode overmoded waveguide into multiple lower-capacity $TE_{10}$ mode rectangular waveguides. The mode-transitioning elbow can provide a high-power bend with a short bend radius, which is not possible with a purely overmoded bend. A mode filter has been designed that is matched to sheathed-helix waveguide and mode transitions not only to the desired $TE_{01}$ mode, but also to the unwanted modes to minimize unwanted mode reflection and maximize absorption while passing the desired mode with minimum attenuation. The components described are sufficient for assembly of overmoded waveguide runs between shipboard combat system elements. A remaining component in the process of being developed is a helix rotary joint for mechanically pointed missile illuminator antennas.

The first complete overmoded waveguide run was recently installed on the roof of APL's Building 11; it connected the prototype DDS transmitter and its phased-array antenna during the Cooperative Engagement Capability Milestone 89 test in August 1989.[1] Figure 22 shows the 60-ft-long system, including helix waveguide, mode-

**Figure 22.** Sixty-foot C-band waveguide run located on the roof of APL's Building 11.

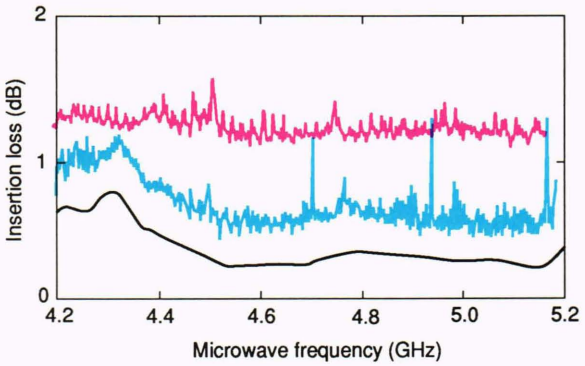


**Figure 23.** Transmission loss versus microwave frequency for the C-band waveguide on the roof of APL's Building 11. The black curve is for a 48-ft circular waveguide and two circular-rectangular transitions; the blue curve is for a 48-ft circular waveguide, two circular-rectangular transitions, a 10-ft WR187 waveguide, and two waveguide/coaxial adapters; and the red curve is for a 60.5-ft WR187 waveguide and two waveguide/coaxial adapters.

transitioning elbows, and Marie transitions, all made at APL. Not only was this the first opportunity to test the technology with a major new combat system element, but the run was of sufficient length to allow direct measurements of the low waveguide loss. Figure 23 indicates the loss with the waveguide, including elbows and transitions, as compared with an equal length of rectangular waveguide. The measured attenuation is consistent with theory and previous indirect measurements. The advantage of overmoded waveguide relative to rectangular waveguide becomes more dramatic for longer lengths, and the predominant loss for this length is due to the Marie transitions; only a very small portion of the loss is contributed by the helix waveguide. Even lower loss would be expected for high-power applications in which multiple-port transitions replace Marie transitions.

Currently, we are transferring this prototype technology to manufacturable form by refining and simplifying the fabrication processes. Testing to determine additional design requirements for a military-qualified hardened version of these elements is also being pursued. We are coordinating initial efforts with the Naval Weapon Support Center, Crane, Indiana, which will oversee production and militarization assessments. Follow-on efforts will be aimed at operational system introduction. Technology is also available for commercial licensing, for applications such as satellite ground stations, research facilities using high-power microwave energy, and millimeter-wave applications. The computer-aided-design computer programs and fabrication processes are applicable to the millimeter wavelength.

In summary, overmoded waveguide technology has advanced in the process of developing critical components for expected next-generation ship combat systems.

## REFERENCES


[1] Emch, G. F., "Fleet Air Defense and Technology," *Johns Hopkins APL Tech. Dig.* **11**(1&2), 8–16 (1990).

[2] Southworth, G. C., *Forty Years of Radio Research*, Gordon and Breach, New York, pp. 193–199 (1962).

[3] Karbowiak, A. E., *Trunk Waveguide Communication*, Chapman and Hall, Ltd., London (1965).

[4] Anderson, T. N., "Low Loss Transmission Using Overmoded Waveguide: A Practical 1981 Review of the State of the Art," in *Proc. IEEE Symp. on Advances in Antenna and Microwave Technology*, Philadelphia (1981).

[5] Unger, H. G., "Lined Waveguide," *Bell Syst. Tech. J.* **41**, 745–768 (Mar 1962).

[6] Unger, H. G., "Helix Waveguide Theory and Application," *Bell Syst. Tech. J.* **37**, 1599–1663 (Nov 1958).

[7] *Millimetric Waveguide Systems*, IEE Conference Publication No. 146 (Nov 1976).

[8] Lowenstern, W., Jr., and Dunn, D. A., "On the Feasibility of Power Transmission Using Microwave Energy in Circular Waveguide," *J. Microwave Power* **1**(2), 57–61 (1966).

[9] Krill, J. A., Kernan, W. J., Jesurun, M. M., and Huting, W. A., *High Power Overmoded Waveguide*, Vol. 1–8, JHU/APL FS-90-043 (1990).

[10] Unger, H. G., "Non-Cylindrical Helix Waveguide," *Bell Syst. Tech. J.* **40**, 233–254 (Jan 1961).

[11] Krill, J. A., Jesurun, M. M., and Zinger, W. H., "Computer Aided Design for $TE_{01}$ Mode Circular Waveguide," U.S. Patent Pending (1988).

[12] Lapp, R. H., "Apparatus for Winding Wire onto an Arbor," U.S. Patent 4,809,918 (7 Mar 1989).

[13] Marie, G. R. P., "Mode Transforming Waveguide Transition," U.S. Patent 2,859,412 (4 Nov 1958).

[14] Karbowiak, A. E., "Testing of Circular Waveguides Using a Resonant Cavity Technique," *Proc. IEE* **106B**, Supplement 13, 66–70 (Sep 1959).

[15] Zinger, W. H., and Krill, J. A., "Multiport Rectangular $TE_{10}$ to Circular $TE_{01}$ Mode Transducer Having Pyramidal Shaped Means," U.S. Patent 4,628,287 (9 Dec 1986).

[16] Irzinski, E. P., Krill, J. A., and Zinger, W. H., "Sharp Mode Transducer Bend for Overmoded Waveguide," U.S. Patent 4,679,008 (7 Jul 1987).

[17] Reiter, G., "Generalized Telegraphist's Equation for Waveguides of Varying Cross Section," *Proc. IEE* **106B**, 54–57 (Sep 1959).

[18] Huting, W. A., *Numerical Analysis of Tapered Waveguide Transitions*, Ph.D. Dissertation, The University of Maryland, College Park (Aug 1989).

[19] Huting, W. A., and Webb, K. J., "Numerical Analysis of Rectangular and Circular Waveguide Tapers," *IEEE Trans. Magn.* **MAG-25**, 3095–3097 (1989).

[20] Huting, W. A., and Webb, K. J., "Numerical Solution of the Continuous Waveguide Transition Problem," *IEEE Trans. Microwave Theory Tech.* **MTT-37**, 1802–1808 (1989).

[21] Flugel, H., and Kuhn, E., "Computer-Aided Analysis and Design of Circular Waveguide Tapers," *IEEE Trans. Microwave Theory Tech.* **MTT-36**, 332–336 (1988).

[22] Menzel, M. T., and Stokes, H. K., *User's Guide for the POISSON/SUPERFISH Group of Codes*, LA-UR-87-115, Los Alamos National Laboratory (Jan 1987).

[23] Saad, S. S., Davies, J. B., and Davies, O. J., "Analysis and Design of a Circular $TE_{01}$ Mode Transducer," *IEE J. Microwaves Opt. Acoust.* **1**, 58–62 (Jan 1977).

[24] Krill, J. A., "Air Inlet for Internal Cooling of Overmoded Waveguide," U.S. Patent 4,688,007 (18 Aug 1987).


ACKNOWLEDGMENTS: We are grateful to the following people for their patient and invaluable help during this project: Frank Paraska, Roger Lapp, Henry Smigocki, Leo McKenzie, George Vetticad, Willie J. Lee, Richard E. Rouse, and William H. Zinger of APL; Kevin J. Webb of Purdue University; Lenny van Sant and George Kreeger of the Naval Weapon Support Center, Crane, Indiana; and the late Edward P. Irzinski.

## THE AUTHORS

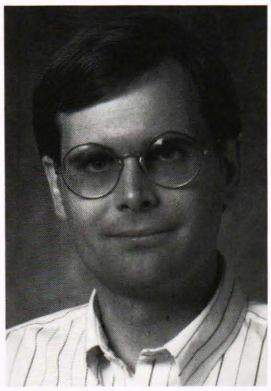

WILLIAM A. HUTING received a B.S.E. in electrical engineering from Duke University in 1981, an M.S.E.E. from the Georgia Institute of Technology in 1982, and a Ph.D. in electrical engineering from The University of Maryland in 1989. From September 1981 to December 1983, he was a Graduate Teaching Assistant with Georgia Tech. Since January 1984, he has been with APL, where he has principally been involved with the development of circular overmoded waveguides and tapered waveguide transitions for use in naval radar systems.

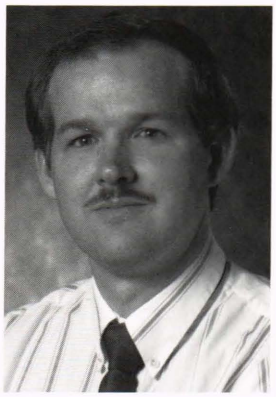

JEFFERY W. WARREN received a B.S. degree in 1982 and an M.S. degree in 1984, both in electrical engineering, from the University of South Carolina. His thesis research evaluated electro-optical measurements of surface charging of insulators in low-frequency electric fields. He joined the Electro-Optical Systems Group in APL's Fleet Systems Department in 1984. Mr. Warren's activities include development and testing of electro-optical systems, and the development of high-power, low-loss, overmoded waveguide.

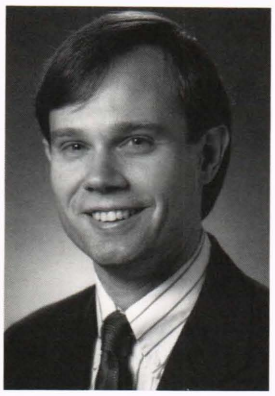

JERRY A. KRILL received B.S. and M.S. degrees in electrical engineering from Michigan State University in 1973 and 1974, respectively, and a Ph.D. in electrical engineering (electrophysics) from The University of Maryland in 1978. He joined the Laboratory in 1973 and is a member of the Principal Professional Staff. Dr. Krill is an Assistant Group Supervisor of the Combat Systems Development Group of the Fleet Systems Department and is also a lecturer in electromagnetics for The Johns Hopkins University Continuing Professional Programs.